

Seasonal Fire Prediction using Spatio-Temporal Deep Neural Networks

Dimitrios Michail* Lefki-Ioanna Panagiotou*

Charalampos Davalas* Ioannis Prapas †

Spyros Kondylatos† Nikolaos Ioannis Bountos*†

Ioannis Papoutsis †

Abstract

With climate change expected to exacerbate fire weather conditions, the accurate anticipation of wildfires on a global scale becomes increasingly crucial for disaster mitigation. In this study, we utilize SeasFire, a comprehensive global wildfire dataset with climate, vegetation, oceanic indices, and human-related variables, to enable seasonal wildfire forecasting with machine learning. For the predictive analysis, we train deep learning models with different architectures that capture the spatio-temporal context leading to wildfires. Our investigation focuses on assessing the effectiveness of these models in predicting the presence of burned areas at varying forecasting time horizons globally, extending up to six months into the future, and on how different spatial or/and temporal context affects the performance of the models. Our findings demonstrate the great potential of deep learning models in seasonal fire forecasting; longer input time-series leads to more robust predictions across varying forecasting horizons, while integrating spatial information to capture wildfire spatio-temporal dynamics boosts performance. Finally, our results hint that in order to enhance performance at longer forecasting horizons, a larger receptive field spatially needs to be considered.

1 Introduction

Fire plays a pivotal role in the Earth system, significantly influencing ecosystems worldwide. While traditionally viewed as a carbon-neutral process over the long term, climate change disrupts this balance through the intensification of fire weather conditions, leading to a rise in global fire activity [8]. A feedback loop is created when fires encroach into evergreen forest regions, posing a threat to their

*Harokopio University of Athens, Greece. {michail, epanagiotou, cdavalas}@hua.gr

†OrionLab, National Technical University & National Observatory of Athens, Greece. {iprapas, skondylatos, bountos, ipapoutsis}@noa.gr

role as carbon sinks. This situation triggers the release of stored carbon into the atmosphere, further exacerbating climate change [4]. Moreover, wildfires represent a critical natural hazard with far-reaching consequences for societies worldwide, resulting in loss of life, property, infrastructure, and ecosystem services [17]. Hence, it is imperative to improve our understanding and forecasting capabilities of wildfire phenomena within the Earth system. By doing so, we can formulate effective strategies to mitigate the adverse impacts of wildfires and climate change.

In this study, our objective is to improve our capacity for wildfire prediction, ultimately contributing to the broader mission of safeguarding ecosystems and societies in the face of evolving climate conditions. We accomplish this by applying and testing different deep learning architectures, e.g. Gated Recurrent Units (GRU), Convolutional Long Short-Term Memory (Conv-LSTM), as well as temporally enabled Graph Neural Networks (TGNN) to environmental data. For all these architectures, we study the impact of the spatio-temporal context on the predictive skill of our models, through a series of experiments with different time-series lengths, spatial neighborhoods, and prediction horizons. All source code can be found at <https://github.com/seasFire/seasfire-ml>.

2 Related Work

Wildfires are notoriously hard to model due to the non-linear interactions between the different Earth system processes that affect them [5]. Weather, vegetation and humans interact in evolving ways that contribute in the expansion or suppression of wildfires. Reichstein et al. [21] propose Deep Learning as a method to learn in a data-driven way these complex spatiotemporal interactions that influence wildfires. Several recent studies have used deep learning for wildfire-related use cases [7]. For short-term daily predictions the temporal context is mostly enough, with spatiotemporal models offering little to no advantage [20, 12]. For longer-term predictions, i.e. on subseasonal to seasonal scales, very few works have studied the effect of spatial and temporal context. Joshi et al. [9] use monthly aggregated input to predict burned area using multi-layer neural networks. Li et al. [13] includes the temporal aspect of the input using a temporal attention network on time-series of fire driver variables to predict the burned area over the tropics. Prapas et al. [18] use temporal snapshots of the fire drivers to predict future burned area patterns, defining burned area forecasting as a segmentation task and demonstrating skillful forecasts even two months in advance. An expansion of this [19], leverages teleconnection indices and global input in conjunction with those snapshots, which helps improve long-term skill, but ignores the temporal component of the input variables. Finally, Zhao et al. [25] integrate causality with GNNs to explicitly model the causal mechanism among complex variables via graph learning, and test their models in the European boreal and Mediterranean biome.

In this work, we examine the performance of various Deep Learning models leveraging the spatiotemporal context of varying size to predict the burned

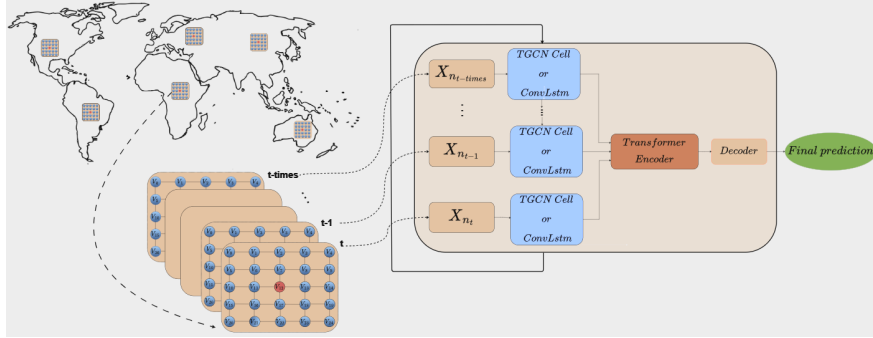


Figure 1: High-level representation of our architecture. The $5 \times 5 \times t$ grid (lower left) represents the structure of the model input. The central (red) vertex is the location in which we try to predict the fire hazard probability. Time t is the time right before the time of the prediction and time $t - times$ is the start time of the time series. X_n stands for the n^{th} sub-graph in the dataset.

area pattern weeks to months in advance, in global scale and at 1° spatial resolution. We do an extensive study to identify optimal sizes for the spatial and temporal context and benchmark different types of architectures including GRUs, temporal GNNs and ConvLSTMs.

3 Seasonal Fire Forecasting

3.1 Dataset

The SeasFire Datacube [10] is an analysis-ready, open-access datacube fit for wildfire forecasting at different spatiotemporal scales. It spans over 21 years (2001-2021) with an 8-day temporal and a 1° spatial resolution (there is also a 0.25° version available). The dataset provides a comprehensive coverage of atmospheric, climatological, vegetation and socioeconomic factors influencing wildfires and contains 58 variables in total, along with target variables, such as burned areas, fire radiative power, and carbon emissions from wildfires.

In this work, we utilized 10 different variables (see Table 1) in order to predict the existence of fire in different time horizons. In addition and when needed, we also used simple positional encodings by augmenting the feature vector with the actual cube coordinates, i.e. \sin/\cos of latitude and longitude. All variables, except the cube coordinates, were standardized before use.

3.2 Problem formulation and methodology

We view the problem as binary classification at a particular location of the cube and a particular timestamp. Thus, given a triplet (ϕ_c, λ_c, t_c) of latitude, longitude and 8-day period we predict whether a fire will occur or not at that

Fullname	Variable name
Mean sea level pressure	mslp
Total precipitation	tp
Vapor Pressure Deficit	vpd
Sea surface temperature	sst
Temperature at 2 meters - Mean	t2m_mean
Surface solar radiation downwards	ssrd
Volumetric soil water level 1	swvl1
Land surface temperature at day	lst_day
Normalized Difference Vegetation Index	ndvi
Population density	pop_dens
Latitude (sin/cos)	cube coordinates
Longitude (sin/cos)	cube coordinates
Target	Variable name
Burned Areas (as binary)	gwis_ba

Table 1: Basic variables (10 input and 2 positional) used for predictions. Target variable represents burned area in hectares (converted to binary).

particular location in time and space. As input we use a timeseries for each variable of length $ts \in \{6, 12, 24, 36\}$ timesteps, where each timestep corresponds to a single 8-day period. As target variable we predict the presence of burned areas at a future timestep $t + h$ with different values of $h \in \{1, 2, 4, 8, 12, 16, 20, 24\}$.

3.2.1 Naive Forecasting

When dealing with seasonal time series, the naive seasonal forecasting method uses the observed values in the same period of the previous seasons [6]. Our dataset encompasses multiple years, enabling the utilization of various baseline methods based on past data. We employ two approaches: Firstly, for forecasting fire occurrence in a specific 8-day period at a given location, we examine historical data to determine if fires were previously recorded in that period at the location. If so, a fire is predicted; otherwise, no fire is predicted. Secondly, using a majority rule, we predict fire occurrence at a location for a specific 8-day period if the number of previous years with fires in that period surpasses the number of years without fires. This majority baseline approach aligns effectively with the binary classification task.

3.2.2 Recurrent Neural Networks

Recurrent Neural Networks [16] are a natural choice when trying to capture temporal dependencies. We utilize a very simple architecture comprising of Gated Recurrent Units [1]. The neural network is comprised of two GRU layers with 64 hidden channels in each layer. A dropout layer with a probability of 0.1

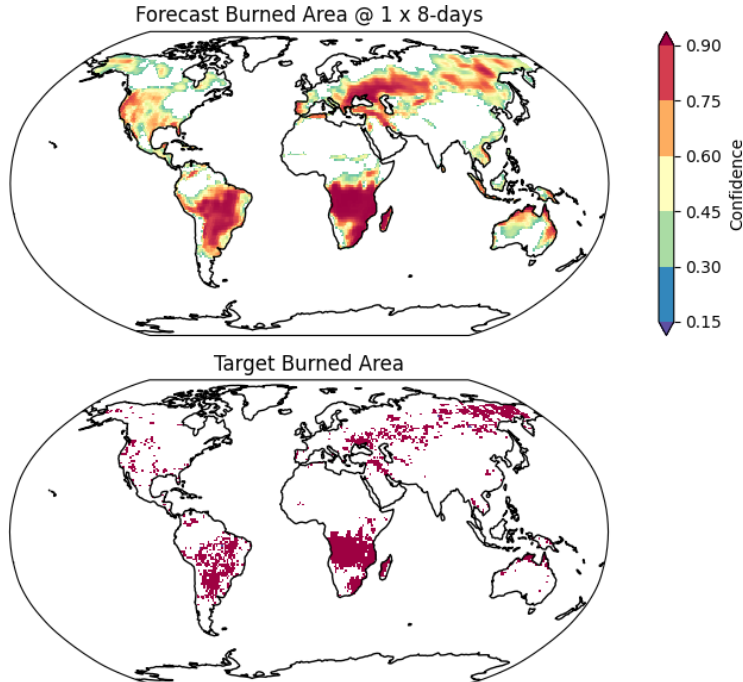


Figure 2: Target variable and prediction of the best global model, using a time-series of length 36, at 07-19-2020. Target is one period (8-days) ahead. Confidence score is the sigmoid output.

exists between the two GRU layers. As the task is binary classification, a final linear layer reduces the representation into a single prediction and a sigmoid function outputs the final prediction.

3.2.3 Convolutional Recurrent Neural Networks

To capture both temporal and spatial dependencies at the same time, we utilize a convolutional LSTM network [22]. In such a network all inputs, cell outputs, hidden states and gates are 3D tensors where the last two dimensions are spatial dimensions (rows and columns). The future state of a certain cell is computed from the input and the past states of its local neighbors. This is achieved by using convolution operators in different transitions such as the state-to-state and/or input-to-state. We utilize a slightly different network from the one in [22]

which is implemented using the following equations:

$$\begin{aligned}
i_t &= \sigma(W_{xi} * X_t + W_{hi} * h_{t-1} + b_i) \\
f_t &= \sigma(W_{xf} * X_t + W_{hf} * h_{t-1} + b_f) \\
o_t &= \sigma(W_{xo} * X_t + W_{ho} * h_{t-1} + b_o) \\
g_t &= \tanh(W_{xg} * X_t + W_{hg} * h_{t-1} + b_g) \\
c_t &= f_t \odot c_{t-1} + i_t \odot g_t \\
h_t &= o_t \odot \tanh(c_t)
\end{aligned}$$

Here $*$ denotes the convolution operator and \odot point-wise

Given (ϕ_c, λ_c) for a particular location of interest and a particular time t we generate a 3D tensor X_t whose last two dimensions are the number of rows and columns of a $(2r+1) \times (2r+1)$ spatial grid. The first dimension is the number of features. The grid is centered at our location of interest while the remaining locations represent $(\phi_c \pm i \cdot 1^\circ, \lambda_c \pm i \cdot 1^\circ)$ for $i \in \{1, \dots, r-1\}$. We feed X_t to the model for each timestep t in order to compute the hidden representation h_t . The final result is obtained by utilizing MultiLayer Perceptron (MLP) layers in order to gradually aggregate the information into a single prediction.

3.2.4 Temporal Graph Convolutional Network

A slightly different approach is to utilize a temporal graph convolutional network model (T-GCN) which combines a graph convolutional network (GNN) and gated recurrent units [24]. Figure 1 shows a high-level representation of the proposed architecture. The GNN is used to capture the topological structure at the location that we are trying to forecast and the GRU captures the temporal dynamics of the environmental information.

Given (ϕ_c, λ_c) for a particular location of interest we generate a small grid graph centered around it depending on a radius $r > 0$ hyper-parameter. Given r the graph contains $(2r+1) \times (2r+1)$ vertices arranged in a spatial grid. The center vertex is our location of interest while the remaining vertices represent locations at $(\phi_c \pm i \cdot 1^\circ, \lambda_c \pm i \cdot 1^\circ)$ for $i \in \{1, \dots, r-1\}$. For each of these vertices we connect it to its k nearest neighbors where again k is a hyper-parameter.

Given the adjacency matrix A of our grid based graph and the feature matrix X , the GCN model can be written as:

$$H^{(l+1)} = \sigma(\tilde{D}^{-\frac{1}{2}} \tilde{A} \tilde{D}^{-\frac{1}{2}} H^{(l)} W^{(l)}),$$

where $\hat{A} = A + I$ is the adjacency matrix of the graph after adding self-loops, \tilde{D} is the degree matrix of the graph with the self-loops, $H^{(l)}$ is the output of the l -th layer, $W^{(l)}$ is the matrix with the trainable parameters of the l -th layer, and $\sigma(\cdot)$ represents the non-linear activation function. A 2-layer GCN model [11] can be expressed as

$$f(A, X) = \sigma(\hat{A} \cdot \text{Relu}(\hat{A} \cdot X \cdot W^{(0)}) \cdot W^{(1)}),$$

where \hat{A} is the normalized adjacency matrix and can be computed in a pre-processing step. Matrices $W^{(0)} \in \mathbb{R}^{d \times h_1}$ and $W^{(1)} \in \mathbb{R}^{h_1 \times h_2}$ are the trainable matrices for the two layers where d is the number of input features and h_1, h_2 the length of the hidden representations. In our experiments we used 64 hidden channels per GCN layer, i.e. $h_1 = h_2 = 64$.

The output of the second layer of the GCN is a hidden representation $h \in \mathbb{R}^{h_2}$ for each vertex of the graph. The T-GCN cell is a GRU cell which given a vertex hidden representation h_{t-1} at timestep $t-1$, produces the output h_t at time t , given the following equations

$$\begin{aligned} u_t &= \sigma(W_u (f_u(A, X_t) \oplus h_{t-1}) + b_u) \\ r_t &= \sigma(W_r (f_r(A, X_t) \oplus h_{t-1}) + b_r) \\ c_t &= \tanh(W_c (f_c(A, X_t) \oplus (r_t \odot h_{t-1})) + b_c) \\ h_t &= u_t \odot h_{t-1} + (1 - u_t) \odot c_t \end{aligned}$$

In the above, \oplus denotes vector concatenation and \odot point-wise multiplication. Note that the model uses different parameters for each of the three GCN models.

The final result is obtained by aggregating the final hidden representations of the T-GCN cells at each graph vertex. Recent works [2, 14] show that using multiple aggregations and learnable aggregations can potentially provide substantial improvements. Therefore, we first apply multi-head self-attention [23] and finally use MLP layers in order to gradually aggregate the information of all vertices to a representation for the entire graph and finally output a single prediction. In our experiments we utilized an attention mechanism with 4 heads and 256 hidden dimension.

4 Experiments

Our methodology can be directly applied to any region of the world, producing different models per region. For our forecasting task, our split is time-based, using years 2002-2017, 2018 and 2019 for train, validation and test respectively. Figure 2 shows the ground truth and the model’s predictions for a specific timestamp, trained to forecast 8 days ahead globally.

Due to our highly imbalanced dataset, the model’s performance is evaluated using the Area Under the Precision-Recall Curve (AUPRC) [3]. We calculate the metric using the average precision score which summarizes a precision-recall curve as a weighted mean of precisions at each threshold, with the difference in recall from the previous threshold as weight

$$AP = \sum_t (R_t - R_{t-1}) \cdot P_t,$$

where P_t, R_t is the respective precision and recall at threshold index t .

Models are trained for 100 epochs. We use binary cross entropy loss and the SGD optimizer. The initial learning rate is set to 0.01 and it adjusted using SGDR [15]. The schedule contains two cycles with 25 and 75 epochs respectively. A weight decay factor of 0.001 is used while training all models.

4.1 Global model

The naive forecasting baseline models discussed in Section 3.2.1 exhibit 0.35 and 0.39 AUPRC. The first baseline checks whether any previous year contains some fire in the same period while the second whether a majority of the previous years contains fires.

Figure 3 presents the best model results when predicting at a global scale. Different GRU, Conv-LSTM and T-GCN models were trained for each different prediction time horizon, resulting in 24 distinct models. Both the Conv-LSTM and the T-GCN model use a radius $r = 5$ resulting in a spatial grid of size 11×11 around the area of interest. The timeseries for all models has a length of 36 8-day periods.

Conv-LSTM starts from 0.74 for the next period prediction, slowly dropping to 0.72 in case of 24 periods. The stability of the prediction, even for large prediction horizons, is mostly due to the large length of the timeseries that is fed to the model. T-GCN starts from 0.69 for the next period prediction which slowly drops to 0.66 when predicting after 24 periods. Similarly, GRU starts from 0.64 down to 0.61.

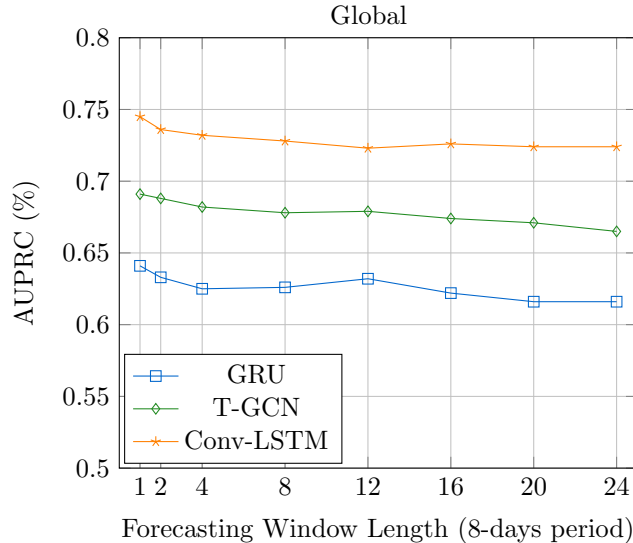


Figure 3: Performance of GRU, Conv-LSTM and T-GCN models at a global scale with timeseries length 36 for different forecasting windows.

4.2 Timeseries length and spatio-temporal context

In this section, we study the effect of training global models with longer or shorter input time series, with or without spatially accumulated information. Figure 4 shows the performance (AUPRC) of the models when trained with

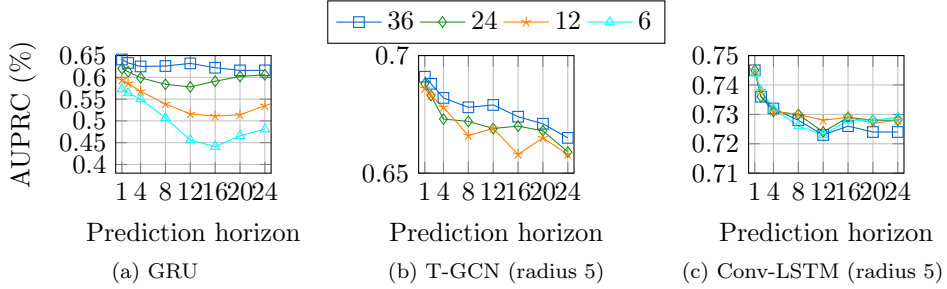


Figure 4: Model performance at a global scale with different time-series length $ts \in \{1, 3, 6, 12, 24, 36\}$ periods (8-days).

four different time-series length $ts \in \{6, 12, 24, 32\}$. For each such length and each forecasting window size $tw \in \{1, 2, 4, 8, 12, 16, 20, 24\}$ we trained a separate model.

Figure 4a contains the results for the GRU models. The first important observation is that the length of the time series is important in order to increase the predictive capabilities of the model. Models which work on input data ranging up to 36 periods (8-day) in the past have better and more stable predictive capabilities and depend less on the sub-seasonality of the input data. This sub-seasonality effect can be observed by the fact that with length 6 time series, the models with target horizons 20 and 24 periods behave slightly better than the models with horizons 12 and 16 periods. This effect is not present when the time-series length is 36 periods. In this case, as expected better performance is achieved when the target horizon is a single 8-day period.

Adding a spatial component to the model while retaining the long-range temporal dependencies seems to improve the prediction instability. Figure 4b show results using the temporal GCN. The graph is constructed using a radius $r = 5$ meaning that the spatial grid-graph has 11×11 vertices. Each vertex is connected to its 9 closest neighbors including itself. We also experimented with other values of r but models with $r = 5$ showed slightly better results. The new models which capture both spatial and temporal aspects improve both the stability of the results, especially for smaller timeseries lengths, but also achieve higher AUPRC. The best GRU model ranged from ≈ 0.61 (target period 24) up to ≈ 0.64 (target period 1) while the TGCN ranged from ≈ 0.66 (target period 24) up to ≈ 0.69 (target period 1). What is also interesting is that the spatial dimension seems to compensate, up to a point, the losses of a smaller timeseries length. When the timeseries length is 12 months, the models up to a target horizon of 8 8-day periods behave similarly to the models with larger timeseries length, i.e. 24 and 36.

Figure 4c contains different Conv-LSTM models. The effect here is stronger. Models with timeseries length 12 (or even 6) achieve identical performance as models trained with larger timeseries.

target	Conv-LSTM (AUPRC)						
	r (radius)						
	1	2	3	4	5	6	7
1	0.726	0.736	0.741	0.742	0.745	0.744	0.743
2	0.720	0.730	0.736	0.739	0.735	0.739	0.739
4	0.714	0.720	0.725	0.728	0.732	0.734	0.735
8	0.708	0.715	0.722	0.724	0.728	0.730	0.731
12	0.703	0.716	0.721	0.724	0.722	0.725	0.729
16	0.702	0.715	0.723	0.726	0.726	0.726	0.726
20	0.707	0.716	0.726	0.725	0.724	0.729	0.727
24	0.710	0.718	0.725	0.727	0.724	0.725	0.729

Table 2: Performance of different Conv-LSTM models for different values of the radius parameter r . Timeseries length is always 36.

4.3 Radius ablation

The radius parameter r affects the receptive field of both the Conv-LSTM and T-GCN models. In both cases the models receive data in a spatial grid of size $(2r + 1) \times (2r + 1)$. When $r = 0$, the situation deteriorates to the case of the GRU model which has access to data from a single location. For larger $r > 0$ the model also receives data from nearby locations. Table 2 contains the performance of separately trained Conv-LSTM models for different values $r > 0$ and different prediction horizons. The results demonstrate that the performance gain from a larger radius, quickly saturates. Recall that for $r = 5$ the spatial grid has size 11×11 , which is already quite large in order to predict only the central location.

4.4 Discussion & Conclusions

Our findings underscore the importance of considering longer time-series data for improving predictive capabilities. We observed that models trained with longer time series, encompassing up to 36 periods (equivalent to an 8-day window), demonstrated superior predictive performance and stability compared to shorter time-series lengths. Particularly, models with longer time-series lengths exhibited reduced dependency on sub-seasonal variations in input data, leading to more robust predictions across varying forecasting horizons. Additionally, the incorporation of a spatial component, further enhanced prediction stability and achieved higher AUPRC, indicating the efficacy of integrating spatial information to capture complex spatiotemporal dynamics inherent in fire prediction tasks.

Furthermore, our study sheds light on the limitations and potential avenues for future research in enhancing the predictive capabilities of deep learning models for fire prediction. Despite the improvements observed with longer time-series data and spatially-aware models, we identified a plateau when trying to

predict over long-range horizons. When the prediction horizon is larger than 12 8-days periods, the model seems to fallback to the average mean cycle performance. This might indicate that the local receptive field of is not enough and we should add long-range teleconnections and additional global information in order to go further in time. In contrast to ConvLSTM, GNNs exhibit notable flexibility in connecting remote nodes, and taking into consideration global information. This ability provides a more comprehensive understanding of intricate patterns and dependencies, making GNNs potentially particularly relevant in scenarios where global context plays a pivotal role.

Acknowledgment

This work has received funding from the SeasFire project, which deals with "Earth System Deep Learning for Seasonal Fire Forecasting" and is funded by the European Space Agency (ESA) in the context of ESA Future EO-1 Science for Society Call.

References

- [1] Kyunghyun Cho, Bart Van Merriënboer, Caglar Gulcehre, Dzmitry Bahdanau, Fethi Bougares, Holger Schwenk, and Yoshua Bengio. Learning phrase representations using rnn encoder-decoder for statistical machine translation. *arXiv preprint arXiv:1406.1078*, 2014.
- [2] Gabriele Corso, Luca Cavalleri, Dominique Beaini, Pietro Liò, and Petar Veličković. Principal neighbourhood aggregation for graph nets. *Advances in Neural Information Processing Systems*, 33:13260–13271, 2020.
- [3] Jesse Davis and Mark Goadrich. The relationship between precision-recall and roc curves. In *Proceedings of the 23rd international conference on Machine learning*, pages 233–240, 2006.
- [4] Mike D Flannigan, Meg A Krawchuk, William J de Groot, B Mike Wotton, and Lynn M Gowman. Implications of changing climate for global wildland fire. *International journal of wildland fire*, 18(5):483–507, 2009.
- [5] Stijn Hantson, Almut Arneth, Sandy P Harrison, Douglas I Kelley, I Colin Prentice, Sam S Rabin, Sally Archibald, Florent Mouillet, Steve R Arnold, Paulo Artaxo, et al. The status and challenge of global fire modelling. *Biogeosciences*, 13(11):3359–3375, 2016.
- [6] Rob J Hyndman and George Athanasopoulos. *Forecasting: principles and practice*. OTexts, 2018.
- [7] Piyush Jain, Sean C.P. Coogan, Sriram Ganapathi Subramanian, Mark Crowley, Steve Taylor, and Mike D. Flannigan. A review of machine learn-

ing applications in wildfire science and management. *Environmental Reviews*, 28(4):478–505, 2020.

- [8] Matthew W Jones, John T Abatzoglou, Sander Veraverbeke, Niels Andela, Gitta Lasslop, Matthias Forkel, Adam JP Smith, Chantelle Burton, Richard A Betts, Guido R van der Werf, et al. Global and regional trends and drivers of fire under climate change. *Reviews of Geophysics*, 60(3):e2020RG000726, 2022.
- [9] Jaideep Joshi and Raman Sukumar. Improving prediction and assessment of global fires using multilayer neural networks. *Scientific reports*, 11(1):3295, 2021.
- [10] Ilektra Karasante, Lazaro Alonso, Ioannis Prapas, Akanksha Ahuja, Nuno Carvalhais, and Ioannis Papoutsis. Seasfire as a multivariate earth system datacube for wildfire dynamics. *arXiv preprint arXiv:2312.07199*, 2023.
- [11] Thomas N Kipf and Max Welling. Semi-supervised classification with graph convolutional networks. *arXiv preprint arXiv:1609.02907*, 2016.
- [12] Spyros Kondylatos, Ioannis Prapas, Michele Ronco, Ioannis Papoutsis, Gustau Camps-Valls, María Piles, Miguel-Ángel Fernández-Torres, and Nuno Carvalhais. Wildfire danger prediction and understanding with deep learning. *Geophysical Research Letters*, 49(17):e2022GL099368, 2022.
- [13] Fa Li, Qing Zhu, William J Riley, Lei Zhao, Li Xu, Kunxiao{jia} Yuan, Min Chen, Huayi Wu, Zhipeng Gui, Jianya Gong, et al. Attentionfire_v1. 0: interpretable machine learning fire model for burned-area predictions over tropics. *Geoscientific Model Development*, 16(3):869–884, 2023.
- [14] Guohao Li, Chenxin Xiong, Ali Thabet, and Bernard Ghanem. Deepgcn: All you need to train deeper gcns. *arXiv preprint arXiv:2006.07739*, 2020.
- [15] Ilya Loshchilov and Frank Hutter. SGDR: stochastic gradient descent with warm restarts. In *5th International Conference on Learning Representations, ICLR 2017, Toulon, France, April 24-26, 2017, Conference Track Proceedings*. OpenReview.net, 2017.
- [16] Larry R Medsker and LC Jain. Recurrent neural networks. *Design and Applications*, 5(64-67):2, 2001.
- [17] M Lucrecia Pettinari and Emilio Chuvieco. Fire danger observed from space. *Surveys in Geophysics*, 41(6):1437–1459, 2020.
- [18] Ioannis Prapas, Akanksha Ahuja, Spyros Kondylatos, Ilektra Karasante, Eleanna Panagiotou, Lazaro Alonso, Charalampos Davalas, Dimitrios Michail, Nuno Carvalhais, and Ioannis Papoutsis. Deep learning for global wildfire forecasting. *arXiv preprint arXiv:2211.00534*, 2022.

- [19] Ioannis Prapas, Nikolaos-Ioannis Bountos, Spyros Kondylatos, Dimitrios Michail, Gustau Camps-Valls, and Ioannis Papoutsis. Televit: Teleconnection-driven transformers improve subseasonal to seasonal wildfire forecasting. In *Proceedings of the IEEE/CVF International Conference on Computer Vision (ICCV) Workshops*, pages 3754–3759, October 2023.
- [20] Ioannis Prapas, Spyros Kondylatos, Ioannis Papoutsis, Gustau Camps-Valls, Michele Ronco, Miguel-Ángel Fernández-Torres, Maria Piles Guillem, and Nuno Carvalhais. Deep learning methods for daily wildfire danger forecasting. *arXiv preprint arXiv:2111.02736*, 2021.
- [21] Markus Reichstein, Gustau Camps-Valls, Bjorn Stevens, Martin Jung, Joachim Denzler, Nuno Carvalhais, and fm Prabhat. Deep learning and process understanding for data-driven earth system science. *Nature*, 566(7743):195–204, 2019.
- [22] Xingjian Shi, Zhourong Chen, Hao Wang, Dit-Yan Yeung, Wai-Kin Wong, and Wang-chun Woo. Convolutional lstm network: A machine learning approach for precipitation nowcasting. *Advances in neural information processing systems*, 28, 2015.
- [23] Ashish Vaswani, Noam Shazeer, Niki Parmar, Jakob Uszkoreit, Llion Jones, Aidan N Gomez, Łukasz Kaiser, and Illia Polosukhin. Attention is all you need. *Advances in neural information processing systems*, 30, 2017.
- [24] Ling Zhao, Yujiao Song, Chao Zhang, Yu Liu, Pu Wang, Tao Lin, Min Deng, and Haifeng Li. T-gcn: A temporal graph convolutional network for traffic prediction. *IEEE transactions on intelligent transportation systems*, 21(9):3848–3858, 2019.
- [25] Shan Zhao, Ioannis Prapas, Ilektra Karasante, Zhitong Xiong, Ioannis Papoutsis, Gustau Camps-Valls, and Xiao Xiang Zhu. Causal graph neural networks for wildfire danger prediction. *arXiv preprint arXiv:2403.08414*, 2024.